



HAL
open science

Experimental determination of the rate constants of the reactions of HO₂ + DO and DO₂+ DO₂

Mohamed Assali, Jozef Rakovsky, Ondrej Votava, Christa Fittschen

► To cite this version:

Mohamed Assali, Jozef Rakovsky, Ondrej Votava, Christa Fittschen. Experimental determination of the rate constants of the reactions of HO₂ + DO and DO₂+ DO₂. International Journal of Chemical Kinetics, 2020, International Journal of Chemical Kinetics, 52 (3), pp.197-206. hal-02992711

HAL Id: hal-02992711

<https://hal.univ-lille.fr/hal-02992711>

Submitted on 6 Nov 2020

HAL is a multi-disciplinary open access archive for the deposit and dissemination of scientific research documents, whether they are published or not. The documents may come from teaching and research institutions in France or abroad, or from public or private research centers.

L'archive ouverte pluridisciplinaire **HAL**, est destinée au dépôt et à la diffusion de documents scientifiques de niveau recherche, publiés ou non, émanant des établissements d'enseignement et de recherche français ou étrangers, des laboratoires publics ou privés.



Experimental Determination of the Rate Constants of the Reactions of HO₂ + DO₂ and DO₂ + DO₂

Journal:	<i>International Journal of Chemical Kinetics</i>
Manuscript ID	KIN-19-0148.R1
Wiley - Manuscript type:	Article
Date Submitted by the Author:	n/a
Complete List of Authors:	Assali, Mohamed; University of Lille Rakovsky, Jozef; J Heyrovsky Institute of Physical Chemistry Czech Academy of Sciences Votava, Ondrej; J Heyrovsky Institute of Physical Chemistry Czech Academy of Sciences Fittschen, Christa; University of Lille
Keywords:	kinetics, HO ₂ radicals, DO ₂ radicals

SCHOLARONE™
Manuscripts

1
2
3
4
5
6
7
8
9
10
11
12
13
14
15
16
17
18
19
20
21
22
23
24
25
26
27
28
29
30
31
32
33
34
35
36
37
38
39
40
41
42
43
44
45
46
47
48
49
50
51
52
53
54
55
56
57
58
59
60

Experimental Determination of the Rate Constants of the Reactions of HO₂ + DO₂ and DO₂ + DO₂

Mohamed Assali¹, Jozef Rakovsky², Ondrej Votava², Christa Fittschen^{1,#}

¹ Université Lille, CNRS, UMR 8522 - PC2A - Physicochimie des Processus de Combustion et de l'Atmosphère, F-59000 Lille, France

² J. Heyrovský Institute of Physical Chemistry v.v.i., Academy of Sciences of the Czech Republic, Dolejškova 3, 18223 Prague, Czech Republic

#Corresponding author: Christa Fittschen (christa.fittschen@univ-lille.fr)
Tel: ++ 33 3 20 33 72 66

Submitted to
International Journal of Chemical Kinetics

Revised version

Abstract

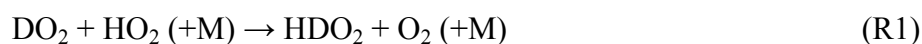
The rate constants of the reactions of $\text{DO}_2 + \text{HO}_2$ (R1) and $\text{DO}_2 + \text{DO}_2$ (R2) have been determined by the simultaneous, selective and quantitative measurement of HO_2 and DO_2 by cw-CRDS in the near infrared, coupled to a radical generation by laser photolysis. HO_2 was generated by photolysing Cl_2 in the presence of CH_3OH and O_2 . Low concentrations of DO_2 were generated simultaneously by adding low concentrations of D_2O to the reaction mixture, leading through isotopic exchange on tubing and reactor walls to formation of low concentrations of CH_3OD and thus formation of DO_2 . Excess DO_2 was generated by photolysing Cl_2 in the presence of CD_3OD and O_2 , small concentrations of HO_2 were always generated simultaneously by isotopic exchange between CD_3OD and residual H_2O . The rate constant k_1 at 295 K was found to be pressure independent in the range 25 – 200 Torr helium, but increased with increasing D_2O concentration $k_1 = (1.67 \pm 0.03) \times 10^{-12} \times (1 + (8.2 \pm 1.6) \times 10^{-18} \text{ cm}^3 \times [\text{D}_2\text{O}] \text{ cm}^{-3}) \text{ cm}^3 \text{ s}^{-1}$. The rate constant for the DO_2 self reaction k_2 has been measured under excess DO_2 concentration, and the DO_2 concentration has been determined by fitting the HO_2 decays, now governed by their reaction with DO_2 , to the rate constant k_1 . A rate constant with insignificant pressure dependence was found: $k_2 = (4.1 \pm 0.6) \times 10^{-13} (1 + (2 \pm 2) \times 10^{-20} \text{ cm}^3 \times [\text{He}] \text{ cm}^{-3}) \text{ cm}^3 \text{ s}^{-1}$ as well as an increase of k_2 with increasing D_2O concentration was observed: $k_2 = (4.14 \pm 0.02) \times 10^{-13} \times (1 + (6.5 \pm 1.3) \times 10^{-18} \text{ cm}^3 \times [\text{D}_2\text{O}] \text{ cm}^{-3}) \text{ cm}^3 \text{ s}^{-1}$. The result for k_2 is in excellent agreement with literature values, while this is the first determination of k_1 .

Introduction

The hydroperoxy radical, HO_2 , is a major radical in oxidation chemistry. In the atmosphere its concentration is closely linked to the OH radical by recycling it through reaction with NO. The self reaction of HO_2 radicals (R3) is a major sink for odd hydrogen in the atmosphere, and presents also the major source of H_2O_2 in the stratosphere. The reaction has attracted a large interest in the last decades and its rate constant presents interesting features such as negative temperature dependence and pressure dependence. Small amounts of water vapor or methanol enhance the rate constant, while addition of NH_3 initially enhances the rate constant but then slows down the reaction at higher concentrations [1],[2],[3],[4],[5],[6],[7],[8],[9],[10],[11]. An extended review on the current knowledge and on the interpretation of this behavior is given by Stone and Rowley [7].

The self reaction of DO_2 , k_2 , shows a similar behavior, but with a rate constant around four times slower than k_3 and the pressure dependence roughly a factor of 2 weaker. The less pronounced pressure dependence for DO_2 compared to HO_2 is attributed to the faster approach to the high pressure limit for DO_2 while the strong kinetic isotope effect has been explained in an early work by Mozurkewich and Benson [4] by using a cyclic transition state instead of the tetraoxide transition state favored by Patrick, Barker and Golden [12]. The six-membered ring complex as transition state has also been confirmed by more recent high level calculations [13],[14].

The rate constant of the cross reaction between the two isotopes HO_2 and DO_2



has never been measured to our knowledge. While this reaction is of no importance in the atmosphere, it might play a role in laboratory experiments, when deuterated compounds are used to elucidate reaction mechanisms [15]. The difficulty in measuring this rate constant is that both isomeric radicals need to be detected in a selective way. In most of the earlier works, HO_2 or DO_2 radicals have been detected by UV-absorption spectroscopy which does not allow a separation between both isomers, because their absorption spectra in the UV range are broad and unstructured. Thrush and Tyndall have in 1982 detected the HO_2 radical selectively in the ν_3 band at 1117 cm^{-1} and have measured the rate constant of the self reaction [16]. Six years later, Martin and Thrush have in 1988 selectively detected the DO_2 radical in the ν_2 band at 1020 cm^{-1} and measured the rate constant of the DO_2 self reaction [17]. However, to our knowledge, no paper has reported so far experiments on the simultaneous, time resolved and selective detection of both isotopes. In the current work, we have used the selective detection of both radicals in the near IR range, where two highly structured absorption ranges can be found: the $2\nu_1$ transition for HO_2 lies at around 6600 cm^{-1} and has been extensively studied and used for its detection [10],[18],[19],[20],[21],[22],[23],[24],[25],[26]. This transition is also used in this work for the quantification of HO_2 . The corresponding DO_2 transition is expected to be around 5000 cm^{-1} [27], but has not been studied to our knowledge, probably due to increased experimental difficulties occurring in this wavelength range compared to 6600 cm^{-1} . Instead, the low-lying electronic transition of the $\tilde{\text{A}} \ ^2\text{A}' \leftarrow \tilde{\text{X}} \ ^2\text{A}''$ 000-000 band at around 7000 cm^{-1} has been studied and used for the detection of DO_2 [15],[28],[29]. Being an electronic transition, the HO_2 radical can be detected in the same wavelength range [29],[30],[31]. **Figure 1** presents a portion of the $\tilde{\text{A}} \ ^2\text{A}' \leftarrow \tilde{\text{X}} \ ^2\text{A}''$ 000-000 spectrum for HO_2 (blue) and DO_2 (red). The transition used in this work for quantifying the DO_2 concentration

has been chosen to be free of interference from HO₂ transitions and is marked with an asterisk.

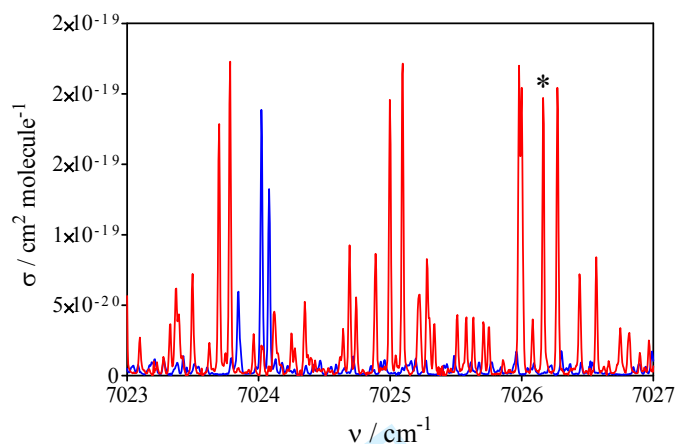


Figure 1: Portion of the HO₂ (blue) and DO₂ (red) spectrum at 25 Torr, adapted from [29]. The line marked with an asterisk indicates the line used in this work for DO₂ quantification.

In this work we present the experimental determination of k_1 , by simultaneous selective detection of both isotopes. The rate constant of the self reaction of DO₂ radicals:



has also been measured. Both rate constant determinations are based on the determination of the absolute HO₂ concentration by fitting HO₂ decays to the well-known rate constant of the HO₂ self reaction, (R3):



In other words, the rate constants k_1 and k_2 have been measured relative to k_3 .

Experimental Section

Experiments have been carried out using pulsed laser photolysis coupled to cw-CRDS. The set-up has been described in detail elsewhere [29,[32],[33],[34] and only a brief description will be given here. The experimental set-up contains two cw-CRDS paths, which cross the photolysis beam symmetrically in a small angle. This allows the simultaneous, time resolved and absolute detection of two species. An overlap between photolysis and detection beam of 37.7cm is obtained. To control if the photolysis laser is well aligned, *i.e.* both cw-CRDS paths sample the same path lengths, HO₂ radicals are detected in an initial experiment on both paths: the retrieved concentrations from both paths agreed to better than 5%.

Experiments have been carried out under either excess HO₂ over DO₂, or excess DO₂ over HO₂. HO₂ was detected on one path for all experiments within the $2\nu_1$ vibrational overtone

band at either the strongest transition at 6638.205 cm⁻¹ or, when HO₂ concentrations were high and absorption became too strong, on a smaller transition at 6638.58 cm⁻¹. DO₂ has been detected on the other path in the $\tilde{A} \ ^2A' \leftarrow \tilde{X} \ ^2A''$ 000-000 band at 7026.16 cm⁻¹.

The reaction is initiated by 351 nm excimer laser photolysis (Lambda Physik, LPX 202i) of Cl₂



The laser fluence was typically 30-40 mJ cm⁻², leading to a photolysis yield of around 1% for Cl₂. HO₂ radicals were generated by the reaction of the Cl-atoms with CH₃OH in the presence of O₂:



For experiments with excess HO₂ over DO₂, low concentrations of DO₂ radicals in the presence of excess HO₂ were generated by adding low concentrations of D₂O to the gas flow. This way, rapid H/D isotope exchange between the labile -OH in CH₃OH and D₂O lead to formation of some CH₃OD which then reacts with Cl [29]:



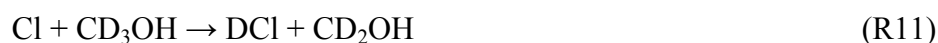
with subsequent formation of DO₂ through



Excess DO₂ over HO₂ was generated through the reaction of Cl atoms with CD₃OD in the presence of O₂:



H₂O, always present in the system, led through H/D exchange always to the formation of some CD₃OH and subsequently to formation of HO₂ through:



In order to decrease the fraction of CD₃OH and thus HO₂, the gas flow was partially saturated with D₂O by flowing a varying fraction of the bath gas Helium through a trap containing liquid D₂O. Concentrations of CH₃OH, CD₃OD and D₂O were estimated from partial pressures and flow rates, no information on the CD₃OH concentration was available, but can be estimated from the HO₂ concentration formed in (R11) and (R12).

(R5) and (R6) are fast ($k_5 = 5.5 \times 10^{-11}$ cm³s⁻¹ and $k_6 = 9.6 \times 10^{-12}$ cm³s⁻¹ [35]), leading with typical concentrations of [CH₃OH] $\approx 8 \times 10^{14}$ cm⁻³ and [O₂] = 1.1×10^{17} cm⁻³ to pseudo-first

order rates of $k_5' = 4.4 \times 10^4 \text{ s}^{-1}$, and $k_6' = 1.1 \times 10^6 \text{ s}^{-1}$, and are thus completed within few 10 μs . No rate constants for the corresponding reactions with the deuterated species are available in the literature, and even though it can be expected that these reactions will be slower due to the kinetic isotope effect, DO_2 will be equally formed on the μs time scale and will be in any case much faster than the peroxy self- and cross-reactions, which take place on the ms time scale. The ratio of $[\text{HO}_2] / [\text{DO}_2]$ is given by the ratio of $k_5 \times [\text{CH}_3\text{OH}] / k_7 \times [\text{CH}_3\text{OD}]$ (or $k_9 \times [\text{CD}_3\text{OD}] / k_{11} \times [\text{CD}_3\text{OH}]$ respectively), whereby the last 2 terms are not known. However, a nearly linear increase of $[\text{DO}_2]$ with increasing $[\text{D}_2\text{O}]$ to the mixture $\text{Cl}/\text{CH}_3\text{OH}/\text{O}_2$ was observed, while the fraction of HO_2 radicals in a mixture $\text{Cl}/\text{CD}_3\text{OD}/\text{O}_2$ decreased very rapidly upon addition of a small flow of D_2O . Examples for both experimental systems are shown in **Figure 2**: the left graph shows the percentage of Cl-atoms being converted to DO_2 in a mixture $\text{Cl}/\text{CH}_3\text{OH}/\text{D}_2\text{O}/\text{O}_2$ as a function of added $[\text{D}_2\text{O}]$, whereby the DO_2 concentration is obtained as the difference in HO_2 concentration before and after addition of D_2O . The right graph shows the percentage of Cl-atoms being converted to HO_2 in a mixture $\text{Cl}/\text{CD}_3\text{OD}/\text{D}_2\text{O}/\text{O}_2$ as a function of $[\text{D}_2\text{O}]$. Here, HO_2 concentrations have been measured directly using the absorption cross sections, DO_2 concentrations have been determined as explained further down.

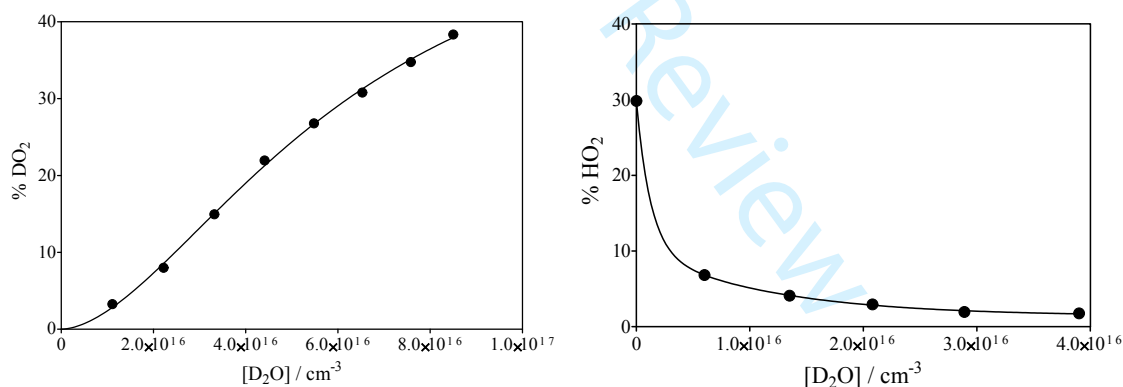


Figure 2: Left graph: Fraction of Cl-atoms converted to DO_2 as a function of added D_2O to a mixture $\text{Cl}/\text{CH}_3\text{OH}/\text{D}_2\text{O}/\text{O}_2$. Total pressure was 50 Torr, $[\text{Cl}]_0 = 1.1 \times 10^{14} \text{ cm}^{-3}$. Right graph: Remaining HO_2 after adding different concentrations of D_2O to a mixture $\text{Cl}/\text{CD}_3\text{OD}/\text{D}_2\text{O}/\text{O}_2$ in order to decrease concomitantly generated HO_2 . Total pressure was 50 Torr, $[\text{Cl}]_0 = 1.0 \times 10^{14} \text{ cm}^{-3}$.

Experiments have been carried out in the pressure range 25 – 200 Torr, and initial $[\text{Cl}]$ concentration varied typically between $5 - 15 \times 10^{13} \text{ cm}^{-3}$. The concentration of the excess isotope (HO_2 or DO_2) was typically in 5-10 times higher than the concentration of the other isotope (DO_2 or HO_2).

The gas flow into the photolysis reactor was controlled using calibrated flowmeters (Tylan FC-260). The main flows consisted of Helium and O₂ and were directly taken from the cylinder (both Alphagaz 2). The precursor Cl₂ was also directly taken from a commercial cylinder (5% Cl₂ in Helium, Alpha Gaz), CH₃OH (CD₃OD) was added to the gas mixture by flowing helium through a bottle containing liquid CH₃OH (CD₃OD) at room temperature, the concentration was estimated from the CH₃OH vapor pressure, the total pressure in the bottle and the measured flow rate. D₂O was either prepared as a mixture (2%) in a 20 l glass balloon and small concentrations were added through flowmeter in case of HO₂-excess experiments or high concentrations were added by flowing a fraction of the main Helium through a bottle containing liquid D₂O for DO₂-excess experiments.

Results and Discussion

Measurement of the rate constant of HO₂ + DO₂

Experiments have been carried out under large excess of HO₂ over DO₂. Under these conditions, the decay of the excess HO₂ is nearly exclusively governed by the rate constant for its self-reaction k_3 , while for the DO₂ radical the self-reaction plays only a minor role due to lower concentrations and to a lower rate constant of the self-reaction k_2 . Therefore, the DO₂ decay is governed nearly exclusively by their reaction with excess HO₂; *i.e.* by the rate constant k_1 and the absolute concentration of the HO₂ radical. These experimental conditions therefore result in a reliable determination of the rate constant of the cross reaction k_1 , if the absolute HO₂ concentration can be determined. This is possible not only by converting the absorption-time profiles into concentration-time profiles using the well-known absorption cross sections [10],[21],[22],[23],[25],[26], but also by fixing k_3 to the recommended literature value and subsequently adjusting the initial HO₂ concentration to best fit the HO₂ decay: both methods have been applied independently and led always to initial HO₂ concentration agreeing to better than +/-10% (see below). In other words: by choosing excess HO₂ concentration conditions, the rate constant k_1 is measured relative to the well-known rate constant of the HO₂ self-reaction k_3 . Any uncertainties in the absorption cross sections of HO₂ and DO₂ (the absorption lines are very narrow, especially at low pressure, and a small drift in the wavelength emitted by the DFB laser will result in a change of the effective absorption cross section) will not impact the retrieved rate constants k_1 : the HO₂ absorption cross section is refined for each experiment by fitting the HO₂ decays to the fixed k_3 , while the absolute

1
2
3 value of the absorption cross section of DO_2 has only a very minor impact for retrieving k_1 .
4 These conditions minimize the uncertainty on k_1 , because even if cross sections and pressure
5 broadening factors of several strong absorption lines in the $2\nu_1$ transition of HO_2 have been
6 well studied [10],[21],[22],[23],[25],[26], the rather small line at 6638.58 cm^{-1} , that was used in
7 this work in order to avoid saturation of the absorption due to the high initial radical
8 concentrations, is less well known.
9
10
11
12
13

14
15 **Figure 3** shows a typical experiment at 50 Torr helium: the black trace shows the HO_2 profile
16 of an experiment in the absence of D_2O , the green trace shows the HO_2 profile measured
17 under the same conditions, but after addition of a small flow of D_2O to the gas flow; the red
18 trace shows the corresponding DO_2 profile measured simultaneously on the second cw-CRDS
19 path. In a first step, the HO_2 absorption profile in absence of D_2O is fitted to the literature
20 value for the rate constant of the self-reaction, k_3 , using a custom-designed Labview based
21 program. This way the absorption cross section of HO_2 can be retrieved at the given pressure.
22 This step (measuring HO_2 profiles in absence of D_2O) is carried out at each pressure only for
23 some Cl_2 concentrations. In this work, we have used the rate constant for k_3 in helium from
24 Sander *et al* [1]. They have measured the pressure dependence of k_3 for different bath gases
25 (He, Ar, N_2 , O_2 and SF_6) and their value for air (ie. $0.2 \times k_{3,\text{O}_2} + 0.8 \times k_{3,\text{N}_2}$) is in excellent
26 agreement with recommended values from IUPAC [36]. The reliability of k_3 is estimated by
27 the IUPAC committee to be $\pm 40\%$. Because all results in this work are determined relative to
28 k_3 , this uncertainty of $\pm 40\%$ needs to be considered also for our k_1 and k_2 measurements.
29 However, in what follows, we will only consider uncertainties occurring from our
30 measurements and not add the uncertainty of k_3 .
31
32
33
34
35
36
37
38
39
40
41
42

43 Once the HO_2 concentration (and with this the absorption cross section) in absence of DO_2
44 has been determined, the HO_2 absorption time profile in presence of D_2O at the same Cl_2
45 concentration is converted to a concentration-time profile using that absorption cross section.
46 Now, the initial DO_2 concentration can be calculated as the difference between both HO_2
47 concentrations and hence the DO_2 absorption cross section at the given pressure can be
48 determined from the absorption at $t = 0$ s. Finally, the rate constant k_1 is adjusted to best fit the
49 DO_2 profile.
50
51
52
53
54
55
56
57
58
59
60

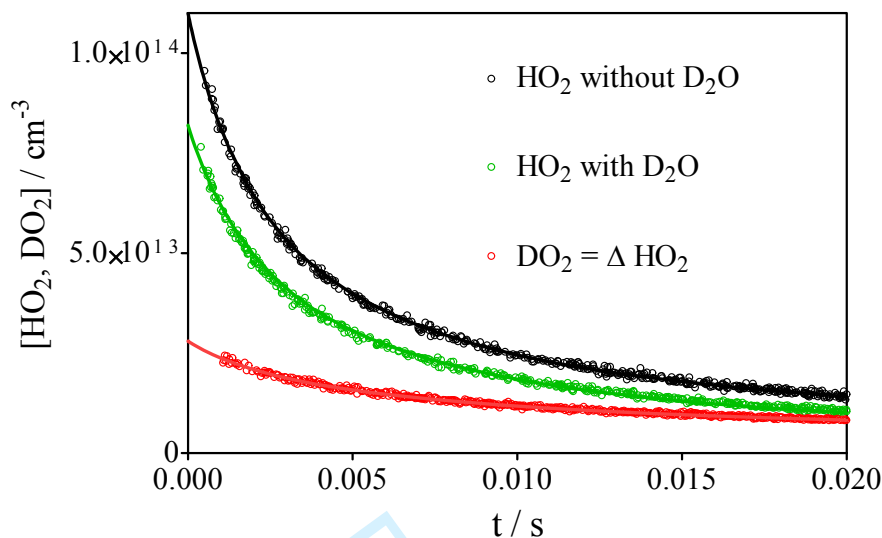


Figure 3: HO₂ concentration time profiles at 50 Torr in absence (black) and presence (green) of D₂O and corresponding DO₂ profile (red) measured simultaneously (*i.e.* the red trace is not the difference between black and green). Initial HO₂ concentrations have been retrieved by fitting decay kinetics using $k_3 = 1.58 \times 10^{-12} \text{ cm}^3\text{s}^{-1}$ [1], initial DO₂ concentration has been normalized as the difference in HO₂ concentration, the DO₂ decay has been fitted by adjusting k_1 .

In practice, for retrieving the rate constant k_1 , the HO₂ and DO₂ absorption profiles for a series of experiments at different Cl₂ concentrations (typically 6 at each pressure, see below) have initially all been converted to concentration-time profiles using the same absorption cross section obtained such as described above. However, HO₂ absorption lines are narrow, and a very minor deviation of the near IR-laser wavelength between different experiments can lead to a variation in the absorption cross section, especially for the low pressure experiments. Therefore, all 6 HO₂ and DO₂ concentration-time profiles have been fitted simultaneously using a very small mechanism consisting of (R1), (R2) and (R3) plus small losses due to diffusion of the radicals out of the photolysis volume. Unique rate constants for all reactions have been used for all different Cl-concentrations at each pressure. The individual HO₂ decays are very sensitive to the initial concentration (see below) and have been finely adjusted to best fit the unique rate constant k_3 . The correction for the individual absorption cross sections was less than 10% for all experiments. The values for the absorption cross sections for HO₂, averaged for each pressure over all experiments, and DO₂ obtained such as described above, are summarized in **Table 1**. Assuming a Voigt profile of the pressure broadened absorption lines, the integrated line strength and pressure broadening parameter have been determined from the data in **Table 1** with values leading for DO₂ (HO₂) to a line strength of $(6.8 \pm 0.7) \times 10^{-21}$ ($(7.9 \pm 0.8) \times 10^{-22}$) cm and a broadening coefficient of 0.165 (0.06) cm⁻¹/atm.

Table 1: Absorption cross sections of HO₂ and DO₂ for all pressures. Error bars contain only the uncertainty from our measurements, an additional uncertainty of ±40% needs to be considered due to the uncertainty of k_3 [36]

P / Torr	$\sigma_{\text{HO}_2} / 10^{-20} \text{cm}^2$ at 6638.58 cm ⁻¹	$\sigma_{\text{DO}_2} / 10^{-20} \text{cm}^2$ at 7026.16 cm ⁻¹
25	3.3 ± 0.3	20 ± 2
50	2.8 ± 0.3	13 ± 1
75	2.4 ± 0.2	12 ± 1
100	2.1 ± 0.2	9.3 ± 0.9
150	1.7 ± 0.2	6.3 ± 0.6
200	1.4 ± 0.1	4.5 ± 0.4

This type of experiment has been carried out at each pressure for a series of 6 different initial Cl₂ concentrations. The HO₂ and DO₂ concentrations as well as the sum of both radicals should increase linearly with increasing Cl₂ concentration. **Table 2** shows these data for a series of experiments at 50 Torr, and the values are plotted in **Figure 4**. The increase in radical concentration with Cl₂ is not perfectly linear (dashed line, forced through origin), but a slight saturation can be observed at the highest Cl₂ concentrations. This might be due to a fast reaction such as Cl + CH₂OH ($k = 6.6 \times 10^{-10} \text{cm}^3 \text{s}^{-1}$) [37], that starts to compete to (R6) or (R8) with increasing Cl concentration. Only one determination is available for the rate constant of the reaction Cl + CH₂OH, and such experiments could possibly be designed in a way (varying O₂ concentration at high Cl-concentration) to re-determine this rate constant, but is out of scope of this paper.

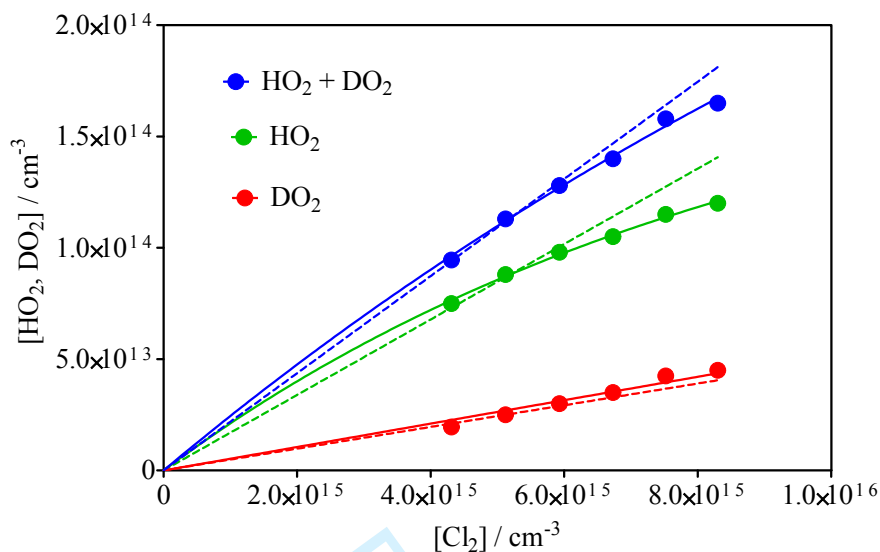


Figure 4: Data from **Table 2**, showing the initial HO_2 (in presence of D_2O), DO_2 and sum of both as a function of Cl_2 concentration

Table 2: Evolution of initial HO_2 (in presence of D_2O) and DO_2 concentration with increasing Cl_2 concentration, the example at 50 Torr

$\text{Cl}_2 / 10^{15} \text{ cm}^{-3}$	$\text{HO}_2 / 10^{14} \text{ cm}^{-3}$	$\text{DO}_2 / 10^{14} \text{ cm}^{-3}$	$\text{HO}_2 + \text{DO}_2 / 10^{14} \text{ cm}^{-3}$
8.30	1.20	0.45	1.65
7.52	1.15	0.43	1.58
6.73	1.05	0.35	1.40
5.93	1.0	0.30	1.28
5.12	0.9	0.25	1.15
4.31	0.8	0.20	1.0

Figure 5 shows a series of HO_2 and DO_2 profiles with different Cl_2 concentrations. For better visibility, the profiles of two intermediate Cl_2 concentrations have been omitted. The full lines show the fit to the simple model containing (R1), (R2) and (R3) as well a loss through diffusion for each radical (very minor impact), using the rate constants from **Table 3**, the inset in the left graph shows a zoom on the HO_2 profiles at short reaction times.

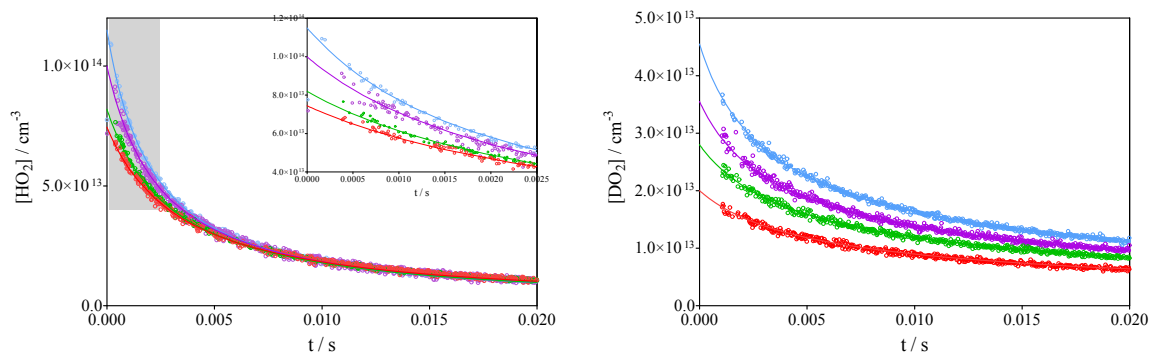


Figure 5: Typical series of experiments with increasing Cl_2 concentration. Left graph: HO_2 profiles, right graph DO_2 profiles. The inset in the left graph shows a zoom of the HO_2 profiles on the first 2.5 ms. No ring-down events occur during the first 1 ms on the DO_2 absorption path, possibly due to perturbation of the DFB laser from scattered 351 nm photons. This phenomena is not observed when using 248 nm photolysis (see [29])

Figure 6 shows the distribution of products for both reaction partners (HO_2 on the left graph, DO_2 on the right graph, green for self-reaction, red for cross reaction) for the experiment with the highest initial radical concentration from **Figure 5**: it can be seen that for HO_2 the self-reaction is the major loss pathway, while for DO_2 self-reaction is very minor and the decay is nearly exclusively governed by its reaction with HO_2 .

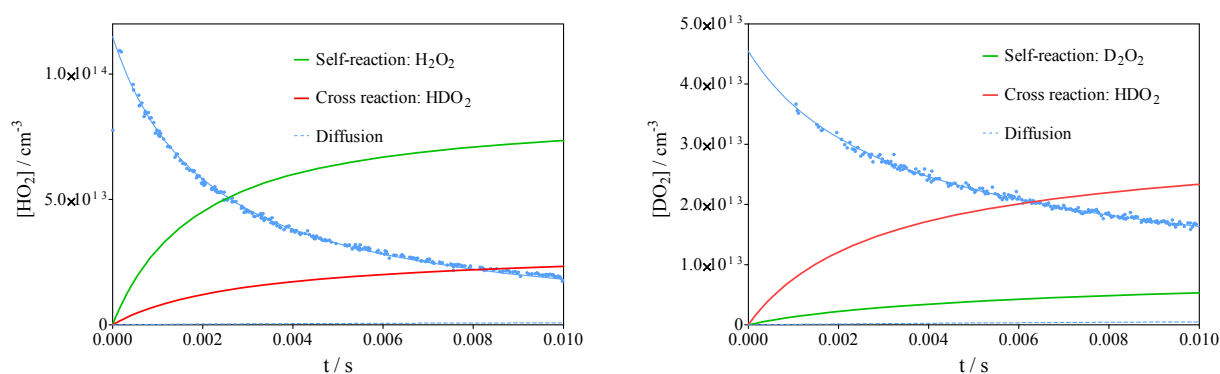


Figure 6: Signal with highest Cl_2 concentration from **Figure 5** with the loss through self-reaction (green line) and cross reaction (red line) for HO_2 (left) and DO_2 (right).

Figure 7 shows the sensitivity of the signals to the rate constant k_1 : the left graph shows both, HO_2 (black) and DO_2 (red), while DO_2 is shown again on the right graph on a zoomed y-scale. The full lines show the best fit using the rate constants from **Table 3** and are barely visible, while for the upper and lower green lines the initial HO_2 concentration in the model has been varied by $\pm 20\%$ (*i.e.* simulating an uncertainty in the HO_2 absorption cross section of $\pm 20\%$). For better visibility, the simulated green curves have been multiplied by 1.2 / 0.8 to match the experimental data, rather than plotting three different experimental curves in which the absorption coefficient $\alpha=f(t)$ would have been converted to $[\text{HO}_2]=f(t)$ using three different absorption cross sections σ . It can be seen that the HO_2 concentration-time profile is not well reproduced anymore with a 20% change in initial concentration, *i.e.* at a fixed rate constant for the HO_2 self reaction, the HO_2 concentration can be determined to better than 20%. At the same time, the 20% change in initial HO_2 concentration leads to a change of the DO_2 concentration-time profile well outside the experimental uncertainty (blue lines).

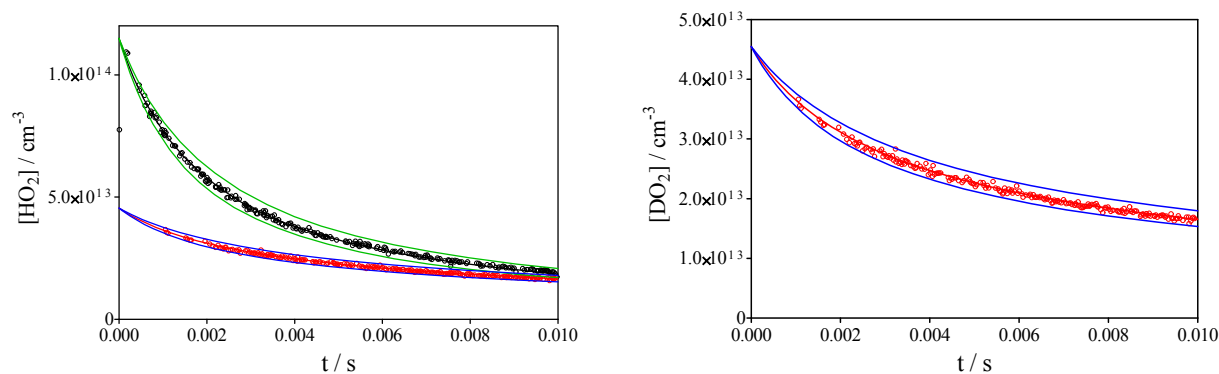


Figure 7: Simulation showing the sensitivity to the initial HO₂ concentration for an experiment at 50 Torr. Black dots: experimental HO₂ concentration time profile, red dots: experimental DO₂ concentration time profile (zoomed in the right graph). Full lines (barely visible): fit to the model of **Table 3**, with the HO₂ concentration adjusted to best fit the decay, lower and upper green lines show variation of HO₂ profile with a +/- 20% change in initial concentration. For visual demonstration of the effect, the simulated green curves have been adapted to match the initial experimental HO₂ concentration, *ie.* have been multiplied by 1.2 / 0.8.

Final results for the rate constants k_1 (and k_2 , see below) for all different pressures are presented in **Figure 9** and **Table 3**. The rate constant for the cross reaction of HO₂ and DO₂ radicals can be given as pressure independent in the range 25 – 200 Torr helium as

$$k_1 = (1.6 \pm 0.3) \times 10^{-12} \text{ cm}^3 \text{ s}^{-1}$$

The error bar includes an uncertainty of 10% from the fitting of the decays and an uncertainty of 10% for the rate constant of the HO₂ self reaction.

Table 3: Rate constants used to fit all experiments. Values k_2 in **bold** are measured in absence of added D₂O, values in *italic* are interpolated. Values for k_3 are calculated from Sander et al. [1] with M = He

P / Torr	k_1 HO ₂ + DO ₂ / 10 ⁻¹² cm ³ s ⁻¹	k_2 DO ₂ + DO ₂ / 10 ⁻¹³ cm ³ s ⁻¹	k_3 HO ₂ + HO ₂ / 10 ⁻¹² cm ³ s ⁻¹	Diffusion / s ⁻¹
25	1.7±0.3	4.0±0.8	1.56	5
50	1.6±0.3	4.1±0.8	1.58	3
75	1.6±0.3	4.2±0.8	1.60	2
100	1.6±0.3	4.3±0.8	1.61	1
150	1.6±0.3	4.4±0.8	1.65	1
200	1.6±0.3	4.5±0.8	1.69	0

Measurement of the rate constant k_2 for the reaction $\text{DO}_2 + \text{DO}_2$

Determining the rate constant for the DO_2 self-reaction, k_3 , requires knowledge of the absolute DO_2 concentration. However, only very little is known about absolute absorption cross sections and pressure broadening in the near infrared [29]. Therefore, two different methods can be used for determining the DO_2 concentration. (a) the Cl-atom concentration is initially determined by adding CH_3OH and thus transforming them quantitatively into HO_2 radicals. After switching to $\text{CD}_3\text{OD}/\text{D}_2\text{O}$ mixtures, the DO_2 and HO_2 absorption time profiles are determined, and the initial DO_2 concentration (and thus the absorption cross section) can be determined under the hypothesis that the Cl-atom concentration has not changed. This is equivalent to the above described method. (b) Fitting the HO_2 decays in presence of excess DO_2 to the reaction system (R1) – (R3) and fixing the rate constant k_1 to the above obtained value. Now the HO_2 decay will depend on the initial DO_2 concentration. Both methods (a) and (b) have been applied independently and have returned values for the initial DO_2 concentrations that agreed to better than 15% to each other. The so-obtained absorption cross section for DO_2 was then used to convert absorption time profiles into absolute DO_2 concentration time profiles, and to determine the rate constant for the DO_2 self-reaction.

In order to minimize the HO_2 concentration that is always formed through (R11) and (R12), D_2O has been added to the gas flow by flowing a fraction of the bath gas Helium through a bubbler containing D_2O . The fraction of Cl-atoms being converted to HO_2 decreased rapidly from around 30% in absence of any added D_2O over 8% in presence of $[\text{D}_2\text{O}] \approx 6 \times 10^{15} \text{ cm}^{-3}$ to less than 2% with $[\text{D}_2\text{O}] \approx 3.5 \times 10^{16} \text{ cm}^{-3}$ (see **Figure 2**).

It was observed that both rate constants, k_1 and k_2 , increased with increasing D_2O concentration, as shown in **Figure 8**. This is in agreement with observations for an increase in k_2 with increasing H_2O concentration.

$$k_1 = (1.67 \pm 0.03) \times 10^{-12} \times (1 + (8.2 \pm 1.6) \times 10^{-18} \text{ cm}^3 \times [\text{D}_2\text{O}] \text{ cm}^{-3}) \text{ cm}^3 \text{ s}^{-1}$$

$$k_2 = (4.14 \pm 0.02) \times 10^{-13} \times (1 + (6.5 \pm 1.3) \times 10^{-18} \text{ cm}^3 \times [\text{D}_2\text{O}] \text{ cm}^{-3}) \text{ cm}^3 \text{ s}^{-1}$$

Error bars represent statistical error only for intercept and an addition error of 10% for uncertainty in the D_2O concentration. The effect observed in this work with D_2O is 2 to 3 times larger than the effect with H_2O , which has been found by Kircher and Sander [2] to be

$$k_3 = 1.6 \times 10^{-12} \times (1 + 2.25 \times 10^{-18} \text{ cm}^3 \times [\text{H}_2\text{O}] \text{ cm}^{-3}) \text{ cm}^3 \text{ s}^{-1}$$

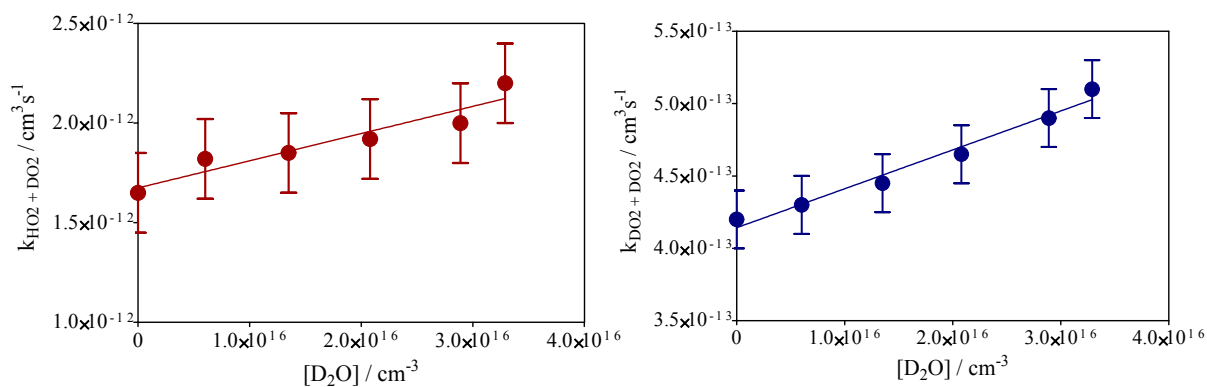


Figure 8: Rate constants k_1 (left) and k_2 (right) as a function of D_2O concentration.

Measurements have been carried out at 50, 100 and 200 Torr (values are given in **bold** in **Table 3**) and insignificant pressure dependence is observed:

$$k_2 = (4.1 \pm 0.6) \times 10^{-13} (1 + (2 \pm 2) \times 10^{-20} \text{ cm}^3 \times [\text{He}] \text{ cm}^{-3}) \text{ cm}^3 \text{ s}^{-1}$$

The error bars represent statistical error only, the systematic error due to the uncertainty in k_3 is not taken into account. The data are plotted in **Figure 9**, together with the values for k_1 as obtained in this work, and k_2 from literature. No data for k_2 in helium could be found in the literature, but extrapolation to $p = 0$ shows a very good agreement of the current results with literature data. Interestingly, in the work of Sander et al, k_2 has been measured at 760 Torr using 2 different precursors: either using Cl_2 photolysis in the presence of $\text{CD}_3\text{OD}/\text{O}_2$ or in the presence of D_2/O_2 . The rate constant they obtained using the first system, was significantly higher than when they used the second system, a difference which was considered by the authors beyond experimental uncertainty and could not be unexplained. A possible explanation would be that in their experiments residual H_2O was also present, which led to some HO_2 next to the desired DO_2 . However, their detection method (UV-absorption spectroscopy) did not allow distinguishing DO_2 from HO_2 , and thus the signal represented the sum of HO_2 and DO_2 and the decay was partially due to the faster reaction of DO_2 with HO_2 . When using D_2 as precursor, no formation of HO_2 is expected, and the observed decay is only due to the slower DO_2 self-reaction.

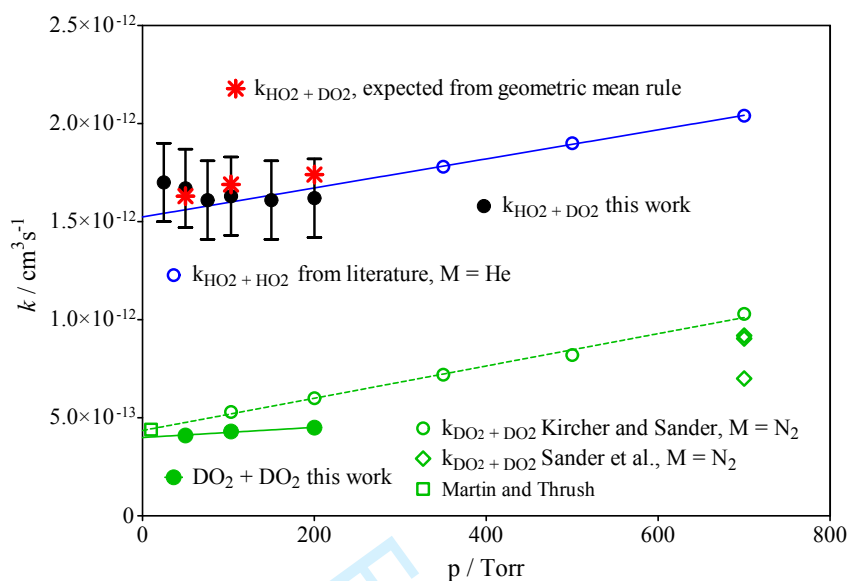


Figure 9: Rate constants k_1 ($\text{HO}_2 + \text{DO}_2$, black dots) and k_2 ($\text{DO}_2 + \text{DO}_2$, green dots) from this work. Literature data for k_2 : open circles from Kircher and Sander [2], open diamonds from Sander *et al.* [1] and open square from Martin and Thrush [17]. Red symbols show k_1 such as expected from geometrical rule, taking k_2 from this work and k_3 from Kircher and Sander [2] (blue symbols).

The geometric mean rule is an empirical approach that allows for the estimation of cross-reaction rate coefficients from the self-recombination rate constants of the reacting partners [38]

$$k_{A+B} = 2 \times \sqrt{k_{A+A} \times k_{B+B}}$$

It has shown to work to better than 20% in the prediction of radical-radicals rate coefficients for a series of hydrocarbon radicals [39]. In absence of any literature data for k_1 , we have tentatively applied this rule to estimate k_1 by using the literature values for k_3 and the values for k_2 such as obtained in this work. In **Figure 9** are shown as red stars the values for k_1 obtained this way: excellent agreement is found with our experimental determinations.

Conclusion

The rate constant of the cross reaction between HO_2 and DO_2 radicals has been measured for the first time thanks to a simultaneous and selective measurement of absolute concentrations of HO_2 and DO_2 radicals by time resolved cw-CRDS in the near infrared. The rate constant was determined under conditions where the HO_2 radical was in excess over the DO_2 radical. Under these conditions, the decay of DO_2 is essentially given by the absolute concentration of HO_2 radicals and the rate constant k_1 . The HO_2 concentration in turn can be determined by

fitting its decay, which is essentially governed by its self-reaction. The rate constant k_1 has been found independent on pressure in the range 25 – 200 Torr helium, but increasing with added D₂O:

$$k_1 = (1.67 \pm 0.03) \times 10^{-12} \times (1 + (8.2 \pm 1.6) \times 10^{-18} \text{ cm}^3 \times [\text{D}_2\text{O}] \text{ cm}^{-3}) \text{ cm}^3 \text{ s}^{-1}$$

The rate constant for the self reaction of DO₂ has been determined by quantifying the DO₂ concentration in two different ways: either Cl-atoms were initially converted to HO₂ radicals (which can be quantified by cw-CRDS) by addition of CH₃OH which can be quantified. Then CH₃OH was replaced by CD₃OD, and it was considered that the Cl-atom concentration had not changed. In an independent method, the decay of the remaining small concentration of HO₂ radicals next to the excess DO₂ radicals was fitted using the above determined rate constant k_1 . Both methods gave consistent concentrations and led to a rate constant with insignificant pressure dependence for the self-reaction of DO₂, in good agreement with the available literature data:

$$k_2 = (4.1 \pm 0.6) \times 10^{-13} (1 + (2 \pm 2) \times 10^{-20} \text{ cm}^3 \times [\text{He}] \text{ cm}^{-3}) \text{ cm}^3 \text{ s}^{-1}$$

For this reaction also, an increase of k_2 with increasing concentration of D₂O was found:

$$k_2 = (4.14 \pm 0.02) \times 10^{-13} \times (1 + (6.5 \pm 1.3) \times 10^{-18} \text{ cm}^3 \times [\text{D}_2\text{O}] \text{ cm}^{-3}) \text{ cm}^3 \text{ s}^{-1}$$

Acknowledgements

This project was supported by the French ANR agency under contract No. ANR-11-Labx-0005-01 CaPPA (Chemical and Physical Properties of the Atmosphere), the Région Hauts-de-France, the Ministère de l'Enseignement Supérieur et de la Recherche (CPER Climibio) and the European Fund for Regional Economic Development. O. Votava and J. Rakovsky thank for financial support through the PHC Barrande project no. 38203PM.

References

1. Sander, S. P.; Peterson, M.; Watson, R. T.; Patrick, R. *J Phys Chem* 1982, 86, 1236-1240.
2. Kircher, C. C.; Sander, S. P. *The Journal of Physical Chemistry* 1984, 88, 2082-2091.
3. Christensen, L. E.; Okumura, M.; Sander, S. P.; Salawitch, R. J.; Toon, G. C.; Sen, B.; Blavier, J. F.; Jucks, K. W. *Geophys. Res. Lett.* 2002, 29, 1299.
4. Mozurkewich, M.; Benson, S. W. *Int J Chem Kinet* 1985, 17, 787-807.
5. Kurylo, M. J.; Ouellette, P. A.; Laufer, A. H. *J Phys Chem* 1986, 90, 437-440.
6. Kanno, N.; Tonokura, K.; Tezaki, A.; Koshi, M. *J Phys Chem A* 2005, 109, 3153-3158.
7. Stone, D.; Rowley, D. M. *PCCP* 2005, 7, 2156 - 2163.
8. Hamilton, E. J.; Lii, R.-R. *Int J Chem Kinet* 1977, 9, 875-885.
9. Lij, R.-R.; Gorse, R. A.; Sauer, M. C.; Gordon, S. *J Phys Chem* 1980, 84, 819-821.
10. Tang, Y.; Tyndall, G. S.; Orlando, J. J. *J Phys Chem A* 2010, 114, 369-378.
11. Kanno, N.; Tonokura, K.; Koshi, M. *J. Geophys. Res.* 2006, 111, D20312.
12. Patrick, R.; Barker, J. R.; Golden, D. M. *The Journal of Physical Chemistry* 1984, 88, 128-136.
13. Zhu, R. S.; Lin, M. C. *PhysChemComm* 2001, 4, 106-111.
14. Donaldson, D. J.; Francisco, J. S. *PCCP* 2003, 5, 3183-3187.
15. Estupiñán, E. G.; Smith, J. D.; Tezaki, A.; Klippenstein, S. J.; Taatjes, C. A. *J Phys Chem A* 2007, 111, 4015-4030.
16. Thrush, B. A.; Tyndall, G. S. *J Chem Soc, Faraday Trans* 1982, 78, 1469-1475.
17. Martin, N. A.; Thrush, B. A. *Chem Phys Lett* 1988, 153, 200-202.
18. Taatjes, C. A.; Oh, D. B. *Appl Opt* 1997, 36, 5817-5821.
19. DeSain, J. D.; Ho, A. D.; Taatjes, C. A. *J Mol Spectrosc* 2003, 219, 163-169.
20. Noell, A. C.; Alconcel, L. S.; Robichaud, D. J.; Okumura, M.; Sander, S. P. *J Phys Chem A* 2010, 114, 6983-6995.
21. Assaf, E.; Liu, L.; Schoemaeker, C.; Fittschen, C. *Journal of Quantitative Spectroscopy & Radiative Transfer* 2018, 211, 107-114.
22. Thiebaud, J.; Crunaire, S.; Fittschen, C. *J Phys Chem A* 2007, 111, 6959-6966.
23. Ibrahim, N.; Thiebaud, J.; Orphal, J.; Fittschen, C. *J Mol Spectrosc* 2007, 242, 64-69.
24. Thiebaud, J.; Aluculesei, A.; Fittschen, C. *J Chem Phys* 2007, 126, 186101.
25. Thiebaud, J.; Fittschen, C. *Appl Phys B* 2006, 85, 383-389.
26. Onel, L.; Brennan, A.; Gianella, M.; Ronnie, G.; Lawry Aguila, A.; Hancock, G.; Whalley, L.; Seakins, P. W.; Ritchie, G. A. D.; Heard, D. E. *Atmos. Meas. Tech. Discuss.* 2017, 10, 4877-4894.
27. Rothman, L. S.; Gordon, I. E.; Babikov, Y.; Barbe, A.; Chris Benner, D.; Bernath, P. F.; Birk, M.; Bizzocchi, L.; Boudon, V.; Brown, L. R.; Campargue, A.; Chance, K.; Cohen, E. A.; Coudert, L. H.; Devi, V. M.; Drouin, B. J.; Fayt, A.; Flaud, J. M.; Gamache, R. R.; Harrison, J. J.; Hartmann, J. M.; Hill, C.; Hodges, J. T.; Jacquemart, D.; Jolly, A.; Lamouroux, J.; Le Roy, R. J.; Li, G.; Long, D. A.; Lyulin, O. M.; Mackie, C. J.; Massie, S. T.; Mikhailenko, S.; Müller, H. S. P.; Naumenko, O. V.; Nikitin, A. V.; Orphal, J.; Perevalov, V.; Perrin, A.; Polovtseva, E. R.; Richard, C.; Smith, M. A. H.; Starikova, E.; Sung, K.; Tashkun, S.; Tennyson, J.; Toon, G. C.; Tyuterev, V. G.; Wagner, G. *J Quant Spectrosc Radiat Transfer* 2013, 130, 4-50.
28. Fink, E. H.; Ramsay, D. A. *J Mol Spectrosc* 2002, 216, 322-334.
29. Assaf, E.; Asvany, O.; Votava, O.; Batut, S.; Schoemaeker, C.; Fittschen, C. *J Quant Spectrosc Radiat Transfer* 2017, 201, 161-170.
30. Fink, E. H.; Ramsay, D. A. *J Mol Spectrosc* 1997, 185, 304-324.
31. Clifford, E. P.; Farrell, J. T.; DeSain, J. D.; Taatjes, C. A. *J Phys Chem A* 2000, 104, 11549-11560.
32. Parker, A.; Jain, C.; Schoemaeker, C.; Szriftgiser, P.; Votava, O.; Fittschen, C. *Appl Phys B* 2011, 103, 725-733.
33. Votava, O.; Masat, M.; Parker, A. E.; Jain, C.; Fittschen, C. *Rev Sci Instrum* 2012, 83, 043110.
34. Assaf, E.; Fittschen, C. *J Phys Chem A* 2016, 120, 7051-7059.

- 1
2
3 35. Atkinson, R. B., D.L.; Cox, R.A.; Crowley, J.N.; Hampson, R.F, Jr.; Kerr, J.A.; Rossi, M.J.; Troe, J.
4 IUPAC Subcommittee on Gas Kinetic Data Evaluation for Atmospheric Chemistry Web Version
5 December 2001 2001, 1 - 56.
6
7 36. Atkinson, R.; Baulch, D. L.; Cox, R. A.; Crowley, J. N.; Hampson, R. F.; Hynes, R. G.; Jenkin, M.
8 E.; Rossi, M. J.; Troe, J. ACP 2004, 4, 1461-1738.
9 37. Pagsberg, P.; Munk, J.; Sillesen, A.; Anastasi, C. Chem Phys Lett 1988, 146, 375-381.
10 38. Jasper, A. W.; Klippenstein, S. J.; Harding, L. B. J Phys Chem A 2007, 111, 8699-8707.
11 39. Klippenstein, S. J.; Georgievskii, Y.; Harding, L. B. PCCP 2006, 8, 1133-1147.
12
13
14
15
16
17
18
19
20
21
22
23
24
25
26
27
28
29
30
31
32
33
34
35
36
37
38
39
40
41
42
43
44
45
46
47
48
49
50
51
52
53
54
55
56
57
58
59
60

For Peer Review